Editors' Suggestion

Current- and Field-Induced Topology in Twisted Nodal Superconductors

Pavel A. Volkov,[1,2,3,*] Justin H. Wilson,[4,1] Kevin P. Lucht,[1] and J. H. Pixley[1,5,6]
[1]Department of Physics and Astronomy, Center for Materials Theory, Rutgers University, Piscataway, New Jersey 08854, USA
[2]Department of Physics, Harvard University, Cambridge, Massachusetts 02138, USA
[3]Department of Physics, University of Connecticut, Storrs, Connecticut 06269, USA
[4]Department of Physics and Astronomy, and Center for Computation and Technology, Louisiana State University, Baton Rouge, Louisiana 70803, USA
[5]Center for Computational Quantum Physics, Flatiron Institute, 162 5th Avenue, New York, New York 10010, USA
[6]Physics Department, Princeton University, Princeton, New Jersey 08544, USA

(Received 5 April 2021; revised 6 December 2022; accepted 13 March 2023; published 4 May 2023)

We show that interlayer current induces topological superconductivity in twisted bilayers of nodal superconductors. A bulk gap opens and achieves its maximum near a "magic" twist angle θ_{MA}. Chiral edge modes lead to a quantized thermal Hall effect at low temperatures. Furthermore, we show that an in-plane magnetic field creates a periodic lattice of topological domains with edge modes forming low-energy bands. We predict their signatures in scanning tunneling microscopy. Estimates for candidate materials indicate that twist angles $\theta \sim \theta_{\mathrm{MA}}$ are optimal for observing the predicted effects.

DOI: 10.1103/PhysRevLett.130.186001

Controlling the Bogoliubov–de Gennes (BdG) excitations in superconductors is crucial for realizing many coveted quantum phases of matter. For example, topologically nontrivial BdG bands [1] hold the promise of hosting exotic Majorana fermion excitations [2] that can be used to perform topological quantum computation [3]. However, despite many considered materials [4–7] and nanostructure setups [8], the controlled realization of topological phases of the BdG quasiparticles remains an open problem. Fundamentally, low-energy BdG quasiparticles are charge neutral combinations of particles and holes [9,10], making the electric-field based control used in various semiconductor applications ineffective.

Recently, a new paradigm in the engineering of correlated and topological phases has emerged, known as "twistronics" [11–13] or moiré materials [14], that uses stacking of two-dimensional materials with an interlayer rotation (i.e., twist as in Fig. 1) to achieve novel properties. In particular, recent studies [15,16] have shown that twisted bilayers of nodal superconductors can spontaneously break time-reversal symmetry at certain twist angles (45° for d-wave superconductors) [17–19], potentially leading to topological states. The cuprates [15] are such a candidate available in monolayer form [20,21]. Recent experiments on interfaces between twisted finite-thickness flakes [22–24] are also consistent with d-wave pairing. However, the topological properties would be suppressed for twist angles near 45° by the symmetry of the orbitals [25] (although incoherent tunneling has been suggested to reduce this effect [26]).

In this Letter, we demonstrate that twisted bilayers of two-dimensional nodal superconductors (TBSCs) (Fig. 1) realize topological phases on application of current or magnetic field at any nonzero twist angle. An interlayer Josephson current opens a topological gap that is maximal at a value of the twist angle much smaller than the one required for spontaneous time-reversal breaking [15,17–19] and is gradually suppressed for large twist angles [Fig. 2(a)]. We also show that an in-plane magnetic field creates a network of topological domains with alternating Chern numbers and chiral edge modes between them [Fig. 3(a)]. We demonstrate the fingerprints of these tunable topological phases in thermal Hall effect [Fig. 2(b)] and local density of states (Fig. 4).

Low-energy model of a twisted nodal superconductor bilayer.—We first construct a momentum space low-energy model of a TBSC [illustrated in Fig. 1(a)]. The relative rotation of the layers is reflected in the single-particle dispersion $\varepsilon(\boldsymbol{K})\tau_3 \to \varepsilon(\boldsymbol{K}^{\mp\theta/2})\tau_3$ and pairing $\Delta(\boldsymbol{K})\hat{\Delta} \to \Delta(\boldsymbol{K}^{\mp\theta/2})\hat{\Delta}$ terms (where $\boldsymbol{K}^{\theta}$ denotes $\boldsymbol{K}$ rotated by θ,

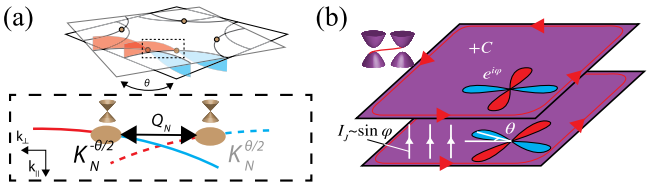

FIG. 1. (a) Momentum-space schematic of a twisted nodal superconductor exemplified by a d-wave superconductor with a sign-changing gap (from blue to red). Near the nodes (K_N and $\tilde{K}_N$) he BdG quasiparticles of the two layers have a Dirac dispersion shifted by a vector $Q_N(=\theta K_N)$ with respect to one another. (b) Interlayer current leads to opening of a bulk $\mathbb{Z}$ topological gap with gapless chiral edge modes (Fig. 2).

and τ_i are Pauli matrices in Gor'kov-Nambu space). Here, we will focus on the singlet case $\hat{\Delta} = \tau_1$ [43]. At low twist angles the twist can be approximated in the vicinity of the nodes by a momentum shift $\tilde{\boldsymbol{K}} \approx \boldsymbol{k}^\theta + [\hat{z} \times \boldsymbol{K}_N]\theta \equiv \boldsymbol{k}^\theta + \boldsymbol{Q}_N$. Assuming that the gap nodes are not in proximity to the Brillouin zone boundary and that the tunneling decays fast outside the first Brillouin zone [43], the interlayer tunneling amplitude can be taken as a constant (t) between overlapping momenta in Fig. 1(a). This implies that the quasiparticles near $\boldsymbol{K}_N$ in one layer can tunnel to a vicinity of only a single corresponding node $\tilde{\boldsymbol{K}}_N$ in the other layer [Fig. 1(b)]. Such pairs of nodes stemming from the two layers form approximately independent "valleys."

At the same time, the setup in Fig. 1(a) constitutes a Josephson junction for weak tunneling. Application of a current lower than a critical one (I_c) between the layers [Fig. 1(b)] therefore creates a phase difference between the order parameters of two layers $\Delta_1 \to \Delta_1 e^{i\varphi/2}$, $\Delta_2 \to \Delta_2 e^{-i\varphi/2}$. The current-phase relation [44] at low twist angles takes the form $I(\varphi) \approx I_c \sin(\varphi)$ [43]. We proceed by neglecting rotation of $\boldsymbol{k}$, which is appropriate for a circular Fermi surface [43] and does not affect qualitative results (see below). The low-energy Hamiltonian of TBSC takes the form $H(\boldsymbol{k}, \varphi) = H_1(\boldsymbol{k}, \varphi) + H_2(\boldsymbol{k}, \varphi)$,

$$\begin{aligned} H_1(\boldsymbol{k}, \varphi) &= v_F k_\parallel \tau_3 + v_\Delta k_\perp \cos(\varphi/2)\tau_1 \\ &\quad - \alpha t \cos(\varphi/2)\tau_1\sigma_3 + t\tau_3\sigma_1 \\ H_2(\boldsymbol{k}, \varphi) &= -v_\Delta k_\perp \sin(\varphi/2)\tau_2\sigma_3 + \alpha t \sin(\varphi/2)\tau_2, \end{aligned} \quad (1)$$

where v_F, v_Δ are the Fermi and gap velocities [$\Delta(K) \approx v_\Delta k_\perp$], $k_\parallel(k_\perp)$ are momenta along $\boldsymbol{v}_F$ ($\boldsymbol{v}_\Delta$), σ_i are Pauli matrices in layer space and $\alpha = (v_\Delta \theta K_N/2t)$. Without current ($\varphi = 0$) $H_2(\boldsymbol{k}, \varphi)$ vanishes, while $H_1(\boldsymbol{k}, \varphi)$ has a gapless spectrum [43]. For $\varphi \neq 0$ a finite spectral gap opens

$$\Delta_J(\varphi) = \begin{cases} 2|t\alpha \sin\varphi/2|, & |\alpha| < \cos\varphi/2 \\ \frac{|t \sin\varphi|}{\sqrt{\alpha^2 + \sin^2\frac{\varphi}{2}}}, & |\alpha| > \cos\varphi/2, \end{cases} \quad (2)$$

for any $\alpha \neq 0$ (i.e., $\theta \neq 0$). The gap vanishes for zero interlayer current $I(\varphi)$, i.e., for $\varphi = 0, \pi$. In Fig. 2(a), we present the maximal value of the current-induced gap $\Delta_J(\varphi = \varphi_{\mathrm{Max}})$ (for φ between 0 and $\pi/2$ corresponding to the stable supercurrent branch) as a function of the twist angle. The maximal gap value is equal to t and is reached at $\theta = \theta_{\mathrm{MA}}/\sqrt{2}$, where $\theta_{\mathrm{MA}} = (2t/v_\Delta K_N)$. To assess the influence of noncircular Fermi surface geometry on the gap we also calculate the spectral gap for a tight-binding Fermi surface appropriate for $Bi_2Sr_2CaCu_2O_{8+y}$ [27,28] [Fig. 2(a), red dots]. The circular Fermi surface approximation (dashed line) is in excellent quantitative agreement at $\theta \ll \theta_{\mathrm{MA}}$. At larger θ, the result can be well-captured by

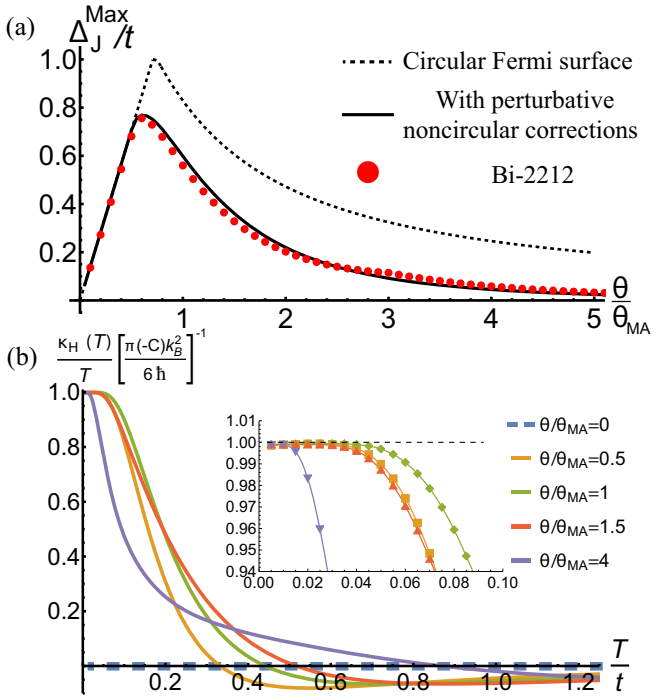

FIG. 2. (a) Maximal value of the current-induced gap as a function of twist angle. Dashed line is for the circular Fermi surface [Eq. (2)]; red dots, for a tight-binding model of $Bi_2Sr_2CaCu_2O_{8+y}$ [27,28]; green line, low-θ expansion for a noncircular Fermi surface [28]. (b) Temperature dependence of the electronic thermal Hall conductivity for different twist angles and $\varphi = \pi/2$. For $\theta = 0$, $\kappa_H(T)$ vanishes identically.

expanding $k^{\pm\theta/2}$ to the lowest order in θ (solid line) [28]. One observes that the gap does not close as a function of twist angle and has an appreciable value for a range of twist angles. For $Bi_2Sr_2CaCu_2O_{8+y}$, the *ab initio* estimates suggest $t \approx 1$ meV [27,28,43], leading to a peak gap value of around 0.8 meV. This value is several times larger than those reported by several other topological superconductivity platforms [45,46].

However, for $\theta \gg \theta_{\mathrm{MA}}$ the gap is strongly suppressed. For example, in $Bi_2Sr_2CaCu_2O_{8+y}$ $\theta_{\mathrm{MA}} \approx 2.8°$ [28,43], which suggests that already at $\theta \approx 15°$ the gap would be below 0.025 meV. In our calculation, we also included the $\propto \cos(2\theta)$ dependence of the interlayer tunneling [28] due to the d-wave symmetry of Cu orbitals [25]. In the clean case, it vanishes for θ close to 45°, where a spontaneous generation of the phase difference was predicted [15,47]. This suggests that the value of the topological gap at low twist angles will be more than an order of magnitude larger than in the vicinity of 45°. The suppression of the gap with θ has been demonstrated also in the presence of strong electronic correlation effects [25], where larger $\theta > 7.8° \approx 2.5\theta_{\mathrm{MA}}$ were studied.

On a qualitative level, the opening of a spectral gap at the nodes in TBSC can be understood to result from a

simultaneous breaking of two symmetries: the mirror symmetry of the bilayer (by the twist) and time-reversal symmetry (by the current). Taking the example of a $d_{x^2-y^2}$ superconductor (relevant for a number of unconventional superconductors [48]), the breaking of these symmetries allows a mixing of the $d_{x^2-y^2}$ and the d_{xy} order parameters with a relative phase between them, i.e., $d_{x^2-y^2} \to d_{x^2-y^2} + e^{i\Phi_{xy}} d_{xy}$. This argument can be similarly generalized to other unconventional superconducting states, i.e., for a triplet p_x superconductor—under a twist and an applied interlayer current a $p_x + ip_y$ topological superconductor emerges [16,43]. The resulting states in all cases are expected to be topological [43,49,50].

To study the topological properties of our system, we rely on the simpler model of Eq. (1) appropriate for $\theta \ll 1$. Let us consider the spectrum near the Dirac points of $H_1(\boldsymbol{k}, \varphi)$ at $\alpha \ll 1$, where $H_2(\boldsymbol{k}, \varphi)$ can be considered as a perturbation. As the gap does not close with increasing α, the topological characteristics apply to all $\alpha \neq 0$. Around $k_\parallel^{\pm} = \pm\sqrt{1-\alpha^2\cos^2(\varphi/2)}\,t/v_F$, $k_\perp = 0$, projecting the Hamiltonian Eq. (1) to the zero-energy eigenstates of $H_1(\boldsymbol{k}, \varphi)$ one obtains two identical Dirac Hamiltonians:

$$H_{\text{eff}} = \tilde{v}_F(\varphi) k_\parallel \zeta_3 + \alpha t \sin\left(\frac{\varphi}{2}\right)\zeta_2 + \tilde{v}_\Delta(\varphi) k_\perp \zeta_1, \qquad (3)$$

where $\tilde{v}_F(\varphi) = \sqrt{1-(\alpha\cos[\varphi/2])^2}$; $\tilde{v}_\Delta(\varphi) = \sqrt{1-(\alpha\cos[\varphi/2])^2}\cos[\varphi/2]$. The Chern number of a single valley with two gapped Dirac points is then equal to ± 1 [51]; the expression valid for arbitrary φ is

$$C = \text{sgn}[v_\Delta \theta \sin(\varphi)]. \qquad (4)$$

Moreover, one can demonstrate that the Chern numbers of different valleys are the same. Consider two adjacent nodes on a single layer's Fermi surface [Fig. 1(a)]. While the Fermi velocity changes smoothly between the two and does not vanish anywhere in between (i.e., v_F does not change sign), v_Δ has to pass through a zero, leading to $v_\Delta \to -v_\Delta$ and $\alpha \to -\alpha$ (after a coordinate rotation) in Eq. (1). Consequently, at the Dirac points in Eq. (3), the last two terms change sign. This results in the Chern number of two adjacent valleys being the same. The total Chern number is then given by $C_{\text{tot}} = N_v C$, where N_v is the number of valleys—equal to the number of nodes in a single layer.

We have proven that the interlayer current transforms nodal TBSCs into a topological state characterized by a $\mathbb{Z}$ topological invariant belonging to the C and D Altland-Zirnbauer symmetry classes [1] for singlet and triplet SCs, respectively. The topological nature of these states produces gapless neutral chiral (Majorana for the equal-spin triplet pairing case) modes at the edges of the system [Fig. 1(b)], expected to result in a quantized electronic

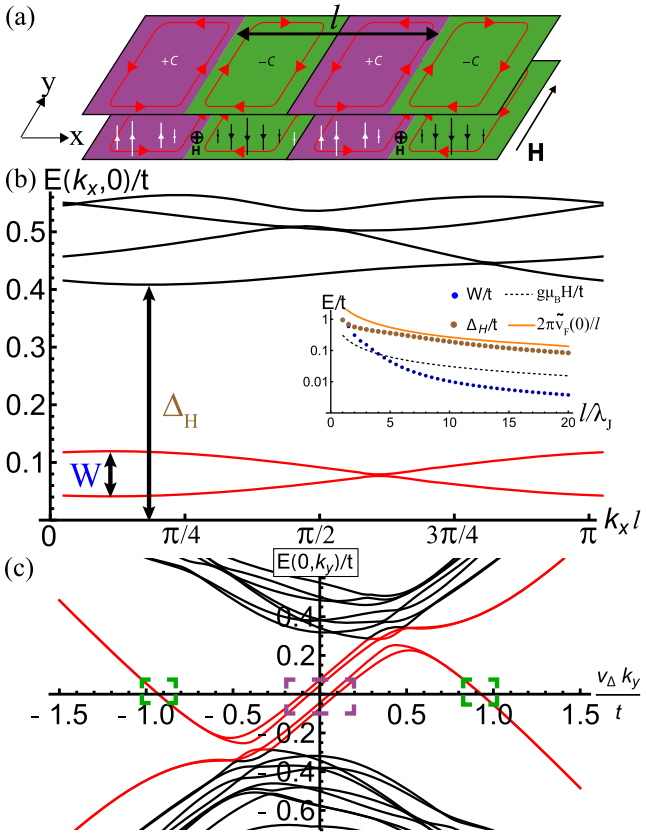

FIG. 3. (a) In-plane magnetic field generates a periodic (along x) Josephson vortex lattice leading to a pattern of gapped domains with edge modes forming bands. (b),(c) Quasiparticle energies along x (b) and y (c) direction in the presence of an in-plane field parallel to $k_\perp$ for $l = 4\lambda_J$. A narrow band (red) is formed within the spectral gap (b). Inset shows the bandwidth W (blue), gap Δ_H (brown), Zeeman energy (black dashed line), and a rough estimate for the gap based on size quantization (orange line) as a function of vortex lattice period l. Dispersion along k_y (c) for $l = 6\lambda_J$ shows the low-energy bands crossing zero with a well-defined chirality. Contributions to the LDOS from the marked momenta are shown in Fig. 4(b). In (b),(c), $\alpha = 0.5$, $(v_F/t\lambda_J) = 0.5$.

thermal (and spin, for the singlet case) Hall conductance $\kappa_H = nT(\pi/6)k_B^2/\hbar$ at low temperatures [49,52], where n is integer. We note that the presence of phonons can modify this prediction, leading to deviations of the quantized value of κ_H/T below a sample-size dependent temperature [53,54].

We have calculated the electronic $\kappa_H(T)$ [28] for Eq. (1) using the expressions in Refs. [55–57]. In Fig. 2(b), we present $\kappa_H(T)$ normalized to $-CT(\pi/6)k_B^2/\hbar$ [28]. For all nonzero twist angles, the quantization occurs, albeit at temperatures considerably lower than the gap. The temperature at which $\kappa_H(T)$ becomes appreciable does not strongly depend on θ, and is around $0.3t$, i.e., 3 K using values appropriate for $Bi_2Sr_2CaCu_2O_{8+\delta}$.

Topological domains induced by an in-plane field.—We now consider the quasiparticles in TBSC in presence of an

in-plane magnetic field instead of a current. Extending the analogy with Josephson junction, one expects the emergence of a periodic modulation of the phase difference and current between layers [58,59]—a lattice of Josephson vortices [Fig. 3(a)]. The alternating current pattern along x [Fig. 4(a)] suggests that quasiparticles should be gapped apart from lines (along y) where the current vanishes and current-induced gap Δ_J changes sign. These lines form domain walls between domains with Chern number equal to $\pm C_{\mathrm{tot}}$.

To study the dispersion of the quasiparticles in the presence of magnetic field, we obtain the BdG Hamiltonian in real space from Eq. (1) by $\varphi \to \varphi(\boldsymbol{r})$, $f(\boldsymbol{r})k_i \to \frac{1}{2}\{(-i\partial_i - e/cA_i(\boldsymbol{r})), f(\boldsymbol{r})\}$ [60], where $\{\cdot,\cdot\}$ denotes the anticommutator. The form of $\varphi(x)$ is determined by the solution of Josephson equations $[\partial^2\varphi(x)/\partial x^2] = (1/\lambda_J^2)\sin\varphi(x)$ [61] (where $\lambda_J^2 = [c|\Phi_0|s'/8\pi^2|j_c|(2\lambda_{ab}^2)]$, λ_{ab} being the penetration depth, $\Phi_0 = (\pi\hbar c/e)$, j_c the critical current density, and s' the thickness of a single layer) [28]. The solution is a periodic function with period $l = \Phi_0/(|H|s)$, where s is the distance between layers and H is the applied field [28]. In addition, for a singlet superconductor, the magnetic field will lead to a Zeeman splitting of $\pm g\mu_B H/2$ for all states [43]. We note that trapped vortices can exist in zero external field [62,63]. This allows one to avoid the Zeeman effect, as the field generated by vortices is negligible for atomically thin bilayers [28].

We will now focus on the case $k_\parallel \| x, k_\perp \| y$, with results for different field orientations being qualitatively similar [28]. k_y remains a good quantum number, while k_x is folded into a Brillouin zone $k_x \in (0, 2\pi/l)$. In Fig. 3(b) an example of the quasiparticle dispersion along x (note that the bands are additionally folded twofold due to the numerical solution procedure [28]). One observes a narrow band inside a gap Δ_H (there is another one at a negative energy). Inset demonstrates that both the width of the narrow band W and the gap Δ_H scale as a function of lattice period l inversely proportional to the magnetic field. At low fields (large l), Josephson vortices are well separated and the quasiparticle energies can be estimated from size quantization of Eq. (3) with $\varphi = 0$, i.e., $\Delta_H \sim [2\pi\tilde{v}_F(0)/l]$. This estimate [see orange line in Fig. 3(b), inset] qualitatively captures the behavior of $\Delta_H(l)$ for a range of l/λ_J. Interestingly, the Zeeman splitting (black dashed line) $(g\mu_B H/t) \approx \{[2\mu_B|\Phi_0|/(s\lambda_J)]/t(l/\lambda_J)\}$ is much smaller than $\Delta_H(l)$ for these parameters [28] and therefore cannot close the gap separating the in-gap band from the rest. The dispersion of the in-gap bands along y direction is shown in red in Fig. 3(c). They cross zero energy and merge with other bands afterwards, reminiscent of the edge states in a topological state.

Indeed, this analogy can be confirmed by analyzing the local density of states (LDOS) at zero energy [Fig. 4(b)]; a quantity that can be measured in scanning tunnel microscopy experiments. We plot the LDOS of one layer of TBSC as in an experiment; only LDOS of the layer closest to the tip will be probed. The position of two peaks in LDOS corresponds exactly to points [Fig. 4(a)], where the current between the layers vanishes. Furthermore, the contributions of states that have opposite chirality [marked by green and purple lines in Fig. 3(b)] are localized at different positions. This confirms the expectation from Fig. 3(a), that the adjacent domain walls host modes moving with opposite velocity along y.

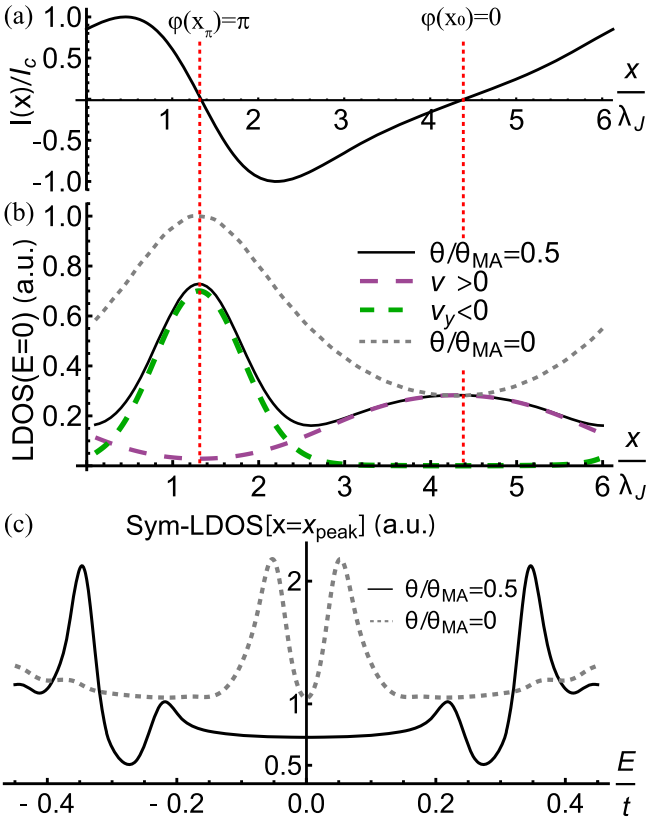

FIG. 4. (a) Interlayer current in the presence of an in-plane field [Fig. 1(d)] over one period $l = 6\lambda_J$ of the Josephson vortex lattice with period. (b) LDOS at zero energy at the top layer. Green and purple lines show contributions of low-energy modes with different chirality [see Fig. 3(b)]. (c) Symmetrized energy dependence of LDOS at the peak position: for finite θ LDOS is constant below within the intra-domain gap.

Additional insight can be obtained by analyzing the Hamiltonian in the vicinity of the points where interlayer current vanishes [Fig. 4(a)]. Taking only the two states closest to zero energy, in analogy to Eq. (3) the Hamiltonian can be brought to the form of a Dirac equation in a linear confining potential [28]:

$$H(x \approx x_0[x_\pi]) = [\alpha]v_F(-i\partial_x)\zeta_3 + [-]v_\Delta k_y\zeta_1 + \frac{\alpha q_{0[\pi]}xt}{2}\zeta_2, \tag{5}$$

where $q_{0,\pi} = \varphi'(x_{0,\pi})$ and the effect of the vector potential has been absorbed into a momentum shift. This Hamiltonian has a localized (in x) solution with a linear dispersion along y $E_{0[\pi](k_y)} = [-]v_\Delta k_y$, in agreement with Fig. 3(c). The spatial extent of the corresponding eigenfunctions $\psi_{0,\pi}(x, k_y)$, i.e., $\sqrt{\langle\psi_{0[\pi]}|(x - x_{0[\pi]})^2|\psi_{0[\pi]}\rangle}$ is independent of k_y and equal to $\sqrt{v_F/(\alpha t q_0)}$ around x_0 and $\sqrt{\alpha v_F/(t q_\pi)}$ around x_π. Noting that $q_\pi > q_0$ and $\alpha < 1$ ψ_π should be localized much stronger, as is indeed the case in Fig. 4(b).

We now compare the results with the case $\theta = 0$, where the topological gap vanishes (Eq. (2)). The spatially resolved zero-energy LDOS has only a single peak [Fig. 4(b)]. More importantly, the LDOS exhibits strikingly different energy dependence [Fig. 4(c)]. In Fig. 4(c), the symmetrized energy dependence of the LDOS at the left peak is shown: for energies within the gap Δ_H, the LDOS is constant for $\theta/\theta_{\mathrm{MA}} = 0.5$, but not for $\theta = 0$, where the spectrum is gapless. This behavior is generic and can be also observed at other positions [28].

Effects of disorder.—Gapped topological states are expected to be robust to weak perturbations [1,52]. To illustrate this general principle we have analyzed Eq. (3) in the presence of a random potential $\langle V_{\mathrm{imp}}(\boldsymbol{r}) V_{\mathrm{imp}}(\boldsymbol{r}')\rangle = n u_0^2$, n being impurity concentration and u_0—scattering strength, in the Born approximation [28]. For $\varphi = 0$, at arbitrarily weak disorder strength, density of states becomes nonzero at zero energy [28,64]. In contrast to that, for a finite φ, DOS remains zero for weak scattering $n u_0^2 \ll 4\pi v_F v_\Delta / \log[\Delta_0/\alpha t \sin(\varphi/2)]$, showing that the topology of the state is robust to weak disorder. In a magnetic field, scattering between edge modes with different v_y could be important. However, their separation in real space [Fig. 4(b)] reduces the scattering rate that is proportional to $|\psi_0(x_{\mathrm{imp}})\psi_\pi(x_{\mathrm{imp}})|^2$, where x_{imp} is the position of the impurity. For parameters used in Fig. 4, one obtains averaging over x_{imp} a factor of 3 reduction compared to scattering between plane waves [28].

Conclusion.—To conclude, we have shown that twisted bilayers of nodal superconductors can realize topological superconductivity of the neutral BdG quasiparticles "on demand" with present-day experimental techniques and systems. Applying an interlayer current bias opens a topological gap in the system that manifests itself in quantized thermal Hall response [Fig. 2(b)]. The gap value is maximized [Fig. 2(a)] near the "magic" value of the twist angle. Similarly, the orbital effect of an in-plane magnetic field creates a network of chiral domains separated by Josephson vortex cores hosting chiral one-dimensional modes [Fig. 3(a)]. With several candidate materials proposed to observe these effects [43], twisted bilayers of nodal superconductors offer a realistic, tunable platform for topological superconductivity.

We thank Philip Kim for insightful discussions. P. A. V., J. H. W., and J. H. P. acknowledge the Aspen Center for Physics where part of this work was performed, which is supported by National Science Foundation Grants PHY-1607611 and PHY-2210452. P. A. V. was supported by a Rutgers Center for Materials Theory Abrahams Fellowship and J. H. P. is partially supported by the Air Force Office of Scientific Research under Grant No. FA9550-20-1-0136, the NSF CAREER Grant No. DMR-1941569, and the Alfred P. Sloan Foundation through a Sloan Research Fellowship. The Flatiron Institute is a division of the Simons Foundation.

*Corresponding author.
pv184@physics.rutgers.edu

[1] A. P. Schnyder, S. Ryu, A. Furusaki, and A. W. W. Ludwig, Classification of topological insulators and superconductors in three spatial dimensions, Phys. Rev. B **78**, 195125 (2008).
[2] M. Sato and Y. Ando, Topological superconductors: A review, Rep. Prog. Phys. **80**, 076501 (2017).
[3] S. D. Sarma, M. Freedman, and C. Nayak, Majorana zero modes and topological quantum computation, npj Quantum Inf. **1**, 15001 (2015).
[4] R. Nandkishore, L. S. Levitov, and A. V. Chubukov, Chiral superconductivity from repulsive interactions in doped graphene, Nat. Phys. **8**, 158 (2012).
[5] F. Liu, C.-C. Liu, K. Wu, F. Yang, and Y. Yao, $d + id'$ Chiral Superconductivity in Bilayer Silicene, Phys. Rev. Lett. **111**, 066804 (2013).
[6] M. H. Fischer, T. Neupert, C. Platt, A. P. Schnyder, W. Hanke, J. Goryo, R. Thomale, and M. Sigrist, Chiral d-wave superconductivity in SrPtAs, Phys. Rev. B **89**, 020509(R) (2014).
[7] P. Zhang *et al.*, Multiple topological states in iron-based superconductors, Nat. Phys. **15**, 41 (2019).
[8] V. Mourik, K. Zuo, S. M. Frolov, S. Plissard, E. P. Bakkers, and L. P. Kouwenhoven, Signatures of Majorana fermions in hybrid superconductor-semiconductor nanowire devices, Science **336**, 1003 (2012).
[9] S. A. Kivelson and D. S. Rokhsar, Bogoliubov quasiparticles, spinons, and spin-charge decoupling in superconductors, Phys. Rev. B **41**, 11693 (1990).
[10] Y. Ronen, Y. Cohen, J.-H. Kang, A. Haim, M.-T. Rieder, M. Heiblum, D. Mahalu, and H. Shtrikman, Charge of a quasiparticle in a superconductor, Proc. Natl. Acad. Sci. U.S.A. **113**, 1743 (2016).
[11] J. M. B. Lopes dos Santos, N. M. R. Peres, and A. H. Castro Neto, Graphene Bilayer with a Twist: Electronic Structure, Phys. Rev. Lett. **99**, 256802 (2007).
[12] R. Bistritzer and A. H. MacDonald, Moiré bands in twisted double-layer graphene, Proc. Natl. Acad. Sci. U.S.A. **108**, 12233 (2011).
[13] S. Carr, D. Massatt, S. Fang, P. Cazeaux, M. Luskin, and E. Kaxiras, Twistronics: Manipulating the electronic properties of two-dimensional layered structures through their twist angle, Phys. Rev. B **95**, 075420 (2017).

[14] L. Balents, C. R. Dean, D. K. Efetov, and A. F. Young, Superconductivity and strong correlations in moiré flat bands, Nat. Phys. **16**, 725 (2020).

[15] O. Can, T. Tummuru, R. P. Day, I. Elfimov, A. Damascelli, and M. Franz, High-temperature topological superconductivity in twisted double-layer copper oxides, Nat. Phys. **17**, 519 (2021).

[16] T. Tummuru, O. Can, and M. Franz, Chiral p-wave superconductivity in a twisted array of proximitized quantum wires, Phys. Rev. B **103**, L100501 (2021).

[17] S. Yip, Josephson current-phase relationships with unconventional superconductors, Phys. Rev. B **52**, 3087 (1995).

[18] K. Kuboki and M. Sigrist, Proximity-induced time-reversal symmetry breaking at Josephson junctions between unconventional superconductors, J. Phys. Soc. Jpn. **65**, 361 (1996).

[19] M. Sigrist, Time-reversal symmetry breaking states in high-temperature superconductors, Prog. Theor. Phys. **99**, 899 (1998).

[20] S. Y. F. Zhao, N. Poccia, M. G. Panetta, C. Yu, J. W. Johnson, H. Yoo, R. Zhong, G. D. Gu, K. Watanabe, T. Taniguchi, S. V. Postolova, V. M. Vinokur, and P. Kim, Sign-Reversing Hall Effect in Atomically Thin High-Temperature $Bi_{2.1}Sr_{1.9}CaCu_{2.0}O_{8+\delta}$ Superconductors, Phys. Rev. Lett. **122**, 247001 (2019).

[21] Y. Yu, L. Ma, P. Cai, R. Zhong, C. Ye, J. Shen, G. D. Gu, X. H. Chen, and Y. Zhang, High-temperature superconductivity in monolayer $Bi_2Sr_2CaCu_2O_{8+\delta}$, Nature (London) **575**, 156 (2019).

[22] S. Y. F. Zhao, N. Poccia, X. Cui, P. A. Volkov, H. Yoo, R. Engelke, Y. Ronen, R. Zhong, G. Gu, S. Plugge, T. Tummuru, M. Franz, J. H. Pixley, and P. Kim, Emergent interfacial superconductivity between twisted cuprate superconductors, arXiv:2108.13455.

[23] J. Lee, W. Lee, G.-Y. Kim, Y.-B. Choi, J. Park, S. Jang, G. Gu, S.-Y. Choi, G. Y. Cho, G.-H. Lee *et al.*, Twisted van der Waals Josephson junction based on a high-T_c superconductor, Nano Lett. **21**, 10469 (2021).

[24] Y. Lee, M. Martini, T. Confalone, S. Shokri, C. N. Saggau, G. Gu, K. Watanabe, T. Taniguchi, D. Montemurro, V. M. Vinokur, K. Nielsch, and N. Poccia, Encapsulating high-temperature superconducting twisted van der Waals heterostructures blocks detrimental effects of disorder, Adv. Mater. 2209135 (2023).

[25] X.-Y. Song, Y.-H. Zhang, and A. Vishwanath, Doping a moiré Mott insulator: A $t-J$ model study of twisted cuprates, Phys. Rev. B **105**, L201102 (2022).

[26] R. Haenel, T. Tummuru, and M. Franz, Incoherent tunneling and topological superconductivity in twisted cuprate bilayers, Phys. Rev. B **106**, 104505 (2022).

[27] R. S. Markiewicz, S. Sahrakorpi, M. Lindroos, H. Lin, and A. Bansil, One-band tight-binding model parametrization of the high-T_c cuprates including the effect of k_z dispersion, Phys. Rev. B **72**, 054519 (2005).

[28] See Supplemental Material at http://link.aps.org/supplemental/10.1103/PhysRevLett.130.186001 for the details of calculations, which includes Refs. [29–42].

[29] I. M. Vishik, W. S. Lee, R.-H. He, M. Hashimoto, Z. Hussain, T. P. Devereaux, and Z.-X. Shen, ARPES studies of cuprate Fermiology: Superconductivity, pseudogap and quasiparticle dynamics, New J. Phys. **12**, 105008 (2010).

[30] A. V. Fedorov, T. Valla, P. D. Johnson, Q. Li, G. D. Gu, and N. Koshizuka, Temperature Dependent Photoemission Studies of Optimally Doped $Bi_2Sr_2CaCu_2O_8$, Phys. Rev. Lett. **82**, 2179 (1999).

[31] M. Kohmoto, Topological invariant and the quantization of the Hall conductance, Ann. Phys. (N.Y.) **160**, 343 (1985).

[32] H. Enriquez, N. Bontemps, A. A. Zhukov, D. V. Shovkun, M. R. Trunin, A. Buzdin, M. Daumens, and T. Tamegai, Penetration of Josephson vortices and measurement of the c-axis penetration depth in $Bi_2Sr_2CaCu_2O_{8+\delta}$: Interplay of Josephson coupling, surface barrier, and defects, Phys. Rev. B **63**, 144525 (2001).

[33] L. N. Bulaevskii, J. R. Clem, and L. I. Glazman, Fraunhofer oscillations in a multilayer system with Josephson coupling of layers, Phys. Rev. B **46**, 350 (1992).

[34] Y. I. Latyshev, J. E. Nevelskaya, and P. Monceau, Dimensional Crossover for Intrinsic dc Josephson Effect in $Bi_2Sr_2CaCu_2O_8$ 2212 Single Crystal Whiskers, Phys. Rev. Lett. **77**, 932 (1996).

[35] Francois Gygi and M. Schlüter, Self-consistent electronic structure of a vortex line in a type-II superconductor, Phys. Rev. B **43**, 7609 (1991).

[36] H. Suematsu, M. Machida, T. Koyama, T. Ishida, and M. Kato, Finite element method for Bogoliubov–de Gennes equation: Application to nano-structure superconductor, Physica (Amsterdam) **412-414C**, 548 (2004).

[37] K. Halterman and O. T. Valls, Local density of states and order parameter configurations in layered ferromagnet-superconductor structures, Physica (Amsterdam) **420C**, 111 (2005).

[38] M. H. Hettler and P. J. Hirschfeld, Scattering by impurity-induced order-parameter "holes" in d-wave superconductors, Phys. Rev. B **59**, 9606 (1999).

[39] T. Pereg-Barnea and M. Franz, Magnetic-field dependence of quasiparticle interference peaks in a d-wave superconductor with weak disorder, Phys. Rev. B **78**, 020509(R) (2008).

[40] A. A. Abrikosov, L. P. Gorkov, and I. E. Dzyaloshinskii, *Quantum Field Theoretical Methods in Statistical Physics* (Pergamon Press, New York, 1965).

[41] P. Van Mieghem, Theory of band tails in heavily doped semiconductors, Rev. Mod. Phys. **64**, 755 (1992).

[42] V. P. Mineev and K. Samokhin, *Introduction to Unconventional Superconductivity* (CRC Press, Boca Raton, 1999).

[43] P. A. Volkov, J.. H. Wilson, K. P. Lucht, and J. H. Pixley, companion paper, Magic angles and correlations in twisted nodal superconductors, Phys. Rev. B **107**, 174506 (2023). In this accompanying article, we provide additional derivation details (including the current-phase relation and effects of the rotation of $\boldsymbol{k}$ by θ, a generalization to triplet pairing) and study the correlated phases near magic angle.

[44] A. A. Golubov, M. Y. Kupriyanov, and E. Il'ichev, The current-phase relation in Josephson junctions, Rev. Mod. Phys. **76**, 411 (2004).

[45] K. Flensberg, F. von Oppen, and A. Stern, Engineered platforms for topological superconductivity and Majorana zero modes, Nat. Rev. Mater. **6**, 944 (2021).

[46] M. Aghaee *et al.*, InAs-Al hybrid devices passing the topological gap protocol, arXiv:2207.02472.

[47] P. A. Volkov, S. Y. F. Zhao, N. Poccia, X. Cui, P. Kim, and J. H. Pixley, Josephson effects in twisted nodal superconductors, arXiv:2108.13456.
[48] G. R. Stewart, Unconventional superconductivity, Adv. Phys. **66**, 75 (2017).
[49] C. Kallin and J. Berlinsky, Chiral superconductors, Rep. Prog. Phys. **79**, 054502 (2016).
[50] S. K. Ghosh, M. Smidman, T. Shang, J. F. Annett, A. D. Hillier, J. Quintanilla, and H. Yuan, Recent progress on superconductors with time-reversal symmetry breaking, J. Phys. Condens. Matter **33**, 033001 (2020).
[51] B. A. Bernevig and T. L. Hughes, *Topological Insulators and Topological Superconductors* (Princeton University Press, Princeton, NJ, 2013).
[52] T. Senthil, J. B. Marston, and M. P. A. Fisher, Spin quantum Hall effect in unconventional superconductors, Phys. Rev. B **60**, 4245 (1999).
[53] Y. Vinkler-Aviv and A. Rosch, Approximately Quantized Thermal Hall Effect of Chiral Liquids Coupled to Phonons, Phys. Rev. X **8**, 031032 (2018).
[54] M. Ye, G. B. Halász, L. Savary, and L. Balents, Quantization of the Thermal Hall Conductivity at Small Hall Angles, Phys. Rev. Lett. **121**, 147201 (2018).
[55] O. Vafek, A. Melikyan, and Z. Tešanović, Quasiparticle Hall transport of *d*-wave superconductors in the vortex state, Phys. Rev. B **64**, 224508 (2001).
[56] H. Sumiyoshi and S. Fujimoto, Quantum thermal Hall effect in a time-reversal-symmetry-broken topological superconductor in two dimensions: Approach from bulk calculations, J. Phys. Soc. Jpn. **82**, 023602 (2013).
[57] V. Cvetkovic and O. Vafek, Berry phases and the intrinsic thermal Hall effect in high-temperature cuprate superconductors, Nat. Commun. **6**, 6518 (2015).
[58] A. Barone and G. Paterno, *Physics and Applications of the Josephson Effect* (Wiley Online Library, New York, 1982), Vol. 1.
[59] M. Tinkham, *Introduction to Superconductivity* (Dover Publications Inc., New York, 1996).
[60] S. H. Simon and P. A. Lee, Scaling of the Quasiparticle Spectrum for *d*-Wave Superconductors, Phys. Rev. Lett. **78**, 1548 (1997).
[61] C. S. Owen and D. J. Scalapino, Vortex structure and critical currents in Josephson junctions, Phys. Rev. **164**, 538 (1967).
[62] A. Ustinov, Solitons in Josephson junctions, Physica (Amsterdam) **123D**, 315 (1998).
[63] H. B. Wang, B. Y. Zhu, C. Gürlich, M. Ruoff, S. Kim, T. Hatano, B. R. Zhao, Z. X. Zhao, E. Goldobin, D. Koelle, and R. Kleiner, Fast Josephson vortex ratchet made of intrinsic Josephson junctions in $Bi_2Sr_2CaCu_2O_8$, Phys. Rev. B **80**, 224507 (2009).
[64] A. V. Balatsky, I. Vekhter, and J.-X. Zhu, Impurity-induced states in conventional and unconventional superconductors, Rev. Mod. Phys. **78**, 373 (2006).